Extraordinarily high fractocohesive lengths in polymer-like networks

Chase M. Hartquist[1,*], Sanketh Challagulla[1], Shu Wang[2], Bolei Deng[3], Gareth H. McKinley[2], and Xuanhe Zhao[2,4,*]

Abstract

The failure resistance of polymer networks dictates their utility as material candidates across industries. However, relating the key length scales driving crack growth to molecular mechanisms remains a key bottleneck in predicting and designing against fracture. The fractocohesive length–defined in terms of the ratio of fracture energy to the specific work to rupture–of a material correlates with the length scale of energy dissipation and controls fracture resistance. Although the Lake-Thomas model predicts the fractocohesive length of a perfect polymer network to match the undeformed mesh size, real soft materials exhibit values that far exceed this prediction. Here we report extraordinarily high fractocohesive lengths in polymer-like networks with and without defects. We find that even perfect networks can have fractocohesive lengths orders of magnitude higher than the undeformed mesh size due to highly nonlinear chain behavior giving rise to nonlocal effects during fracture. Introducing defects further increases the fractocohesive length. We identify quantitative relations between nonlinear chain mechanics, defect length, defect density, and fractocohesive length. Overall, strain-stiffening chain behavior, defect density, and defect size independently correlate with larger fractocohesive lengths in polymer-like networks, and their individual effects can be collapsed into a single power law scaling. These outcomes point the way towards improved physics-informed design of soft yet tough polymers and metamaterials.

Keywords

fractocohesive length, fracture, rupture, polymer-like networks, flaw sensitivity

[1]Department of Mechanical and Aerospace Engineering, University of Florida, Gainesville, FL 32611, USA
[2]Department of Mechanical Engineering, Massachusetts Institute of Technology, Cambridge, MA 02139, USA
[3]Daniel Guggenheim School of Aerospace Engineering, Georgia Institute of Technology, Atlanta, GA 30332, USA
[4]Department of Civil and Environmental Engineering, Massachusetts Institute of Technology, Cambridge, MA 02139, USA

Corresponding authors:

Chase M. Hartquist, Department of Mechanical and Aerospace Engineering, University of Florida, Gainesville, FL 32611, USA. Email: chartquist@ufl.edu

Xuanhe Zhao, Department of Mechanical Engineering, Department of Civil and Environmental Engineering, Massachusetts Institute of Technology, Cambridge, MA 02139, USA. Email: zhaox@mit.edu

Accepted version. Published in *Mathematics and Mechanics of Solids.* (DOI: 10.1177/10812865261420397)

1 Introduction

Elastomers and gels are composed of interconnected networks of polymer chains and form the backbone of many common and advanced materials in the modern world. Their capacity to withstand large, reversible deformations while displaying moduli and fracture properties spanning orders of magnitude make them desirable candidates for applications across the biological, medical, automotive, aerospace, and consumer goods sectors. The fundamental material properties controlling the mechanical failure of soft materials play a pivotal role in determining their value in applications [1–3]. Although theoretical models can accurately predict fracture properties of ductile or brittle materials such as metal and glass [4], existing local or linear frameworks do not fully capture the experimentally observed fracture characteristics of real polymer networks [5–9].

Failure properties of polymer networks are classically measured by two experimental approaches. In the limit of large cracks, the fracture energy Γ describes the energy per unit area (J/m^2) required to advance a crack. It is measured by mechanically loading a sample with a single dominant defect until it propagates. In the limit of small cracks, the specific work to rupture W_{rupture} describes the energy per unit volume (J/m^3) required to break a material. It is measured by uniaxially extending a pristine sample until the material fully separates into multiple parts.

The ratio of the fracture energy and specific work to rupture gives the fractocohesive length scale L_{fc} as [10,11],

$$L_{\text{fc}} = \Gamma / W_{\text{rupture}}. \tag{1}$$

Material-specific length scales in fracture like the fractocohesive length have been used experimentally to measure the crack tip diameter [12,13] and characterize flaw sensitivity [11,14,15] in crystalline and amorphous materials. The Lake-Thomas model defines the fracture energy and specific work to rupture in perfect networks, which correspond to network architectures with uniform topologies, monodisperse chain lengths, and no defects. The fracture energy is given as the energy to dissociate a layer of chains as,

$$\Gamma^{\text{LT}} = M U_{\text{chain}}, \tag{2}$$

where M is the areal density of chains in the undeformed reference state and U_{chain} is the energy to rupture a single chain. The specific work to rupture is provided as the energy density within the network such that,

$$W^{\text{LT}}_{\text{rupture}} = M U_{\text{chain}} / L_0, \tag{3}$$

where L_0 is the undeformed chain length or mesh size. Therefore, the Lake-Thomas model predicts that the fractocohesive length of a perfect network is the original mesh size [16], i.e.,

$$L^{\text{LT}}_{\text{fc}} = L_0. \tag{4}$$

Real polymers typically exhibit fractocohesive lengths that are orders of magnitude higher than their undeformed mesh sizes, which can reach the centimeter scale. Biological tissues [17] and ultratough hydrogels [18,19] display fractocohesive lengths that may be as large as 1-10 cm. Common

polymers like natural rubber[20] and double network gels[21] display fractocohesive lengths of about 0.1 mm. Contributions from sacrificial networks[22–24], chain entanglements[25], hierarchical structures[26,27], strain-induced crystallization[20,28], crosslinking conditions[29], viscoelasticity[30,31], chain dynamics[32], heterogeneities[33], and network imperfection[34] can each enhance the size of the dissipative zone. Understanding the individual molecular and architectural contributions of networks to the fractocohesive length remains a challenging question in the fracture mechanics of stretchable materials.

Here, we implement a polymer-like network model to evaluate computationally the fractocohesive lengths of lattices whose strand mechanical behaviors match those of real flexible polymer chains. We find that perfect polymer-like networks exhibit fractocohesive lengths that are orders of magnitude greater than the undeformed mesh size. The fractocohesive length increases with increasing nonlinearity of the force-extension behavior of polymer chains by promoting nonlocal energy release and dissipation during rupture around the crack tip. Introducing defects further amplifies this effect. Across networks with fixed defect densities, the fractocohesive length increases with defect length, as larger flaws markedly reduce the specific work to rupture. This fracture-modeling approach delivers order-of-magnitude predictive power for the fractocohesive length in polymer-like networks.

2 Methods

Polymer-like networks[35] build on insights from coarse-grained[36–39], mesoscale[40], metamaterial[41], and lattice[42] models by providing an efficient platform to simulate the mechanical response of polymer chains in a crosslinked elastomeric network[43]. Molecular models accounting for entropic elasticity, bond stretching, and chain scission can parametrize experimental single-molecule force spectroscopy (SMFS) measurements of the force-stretch responses from chains of common polymers[44–47]. We adopt the modified freely jointed chain model (m-FJC) to describe the mechanical response of polymer chains within the simulation[45], which relates the force f to the stretch λ through the relationship,

$$\frac{\lambda}{\lambda_{\text{lim}}} = \left[\coth\left(\frac{f}{K_{\text{S}}}\right) - \frac{K_{\text{S}}}{f}\right]\left(1 + \frac{f}{K_{\text{E}}}\right), \tag{5}$$

where K_{S} describes the entropic stiffness, K_{E} describes the energetic stiffness, and λ_{lim} is the transition stretch between these regimes (Fig. 1a). For polymers, K_{E} regularizes the freely-jointed chain model to describe the effect of bond stretching before chain scission. K_{S} defines the thermal response as $k_{\text{B}}\theta/b$, where k_{B} is the Boltzmann constant, θ is the absolute temperature, and b is the length of a Kuhn monomer. λ_{lim} is the chain stretch at the contour length nb (i.e., $\lambda_{\text{lim}} = nb/L_0$), where n is the number of Kuhn monomers in a polymer chain. Prior works have characterized these values based on SMFS experiments with common polymers[48–53]. Historically, Lake and Thomas considered that the energy required to rupture a chain corresponds to the chemical energy U_{mon} needed to break each of the covalent bonds between the N Kuhn monomers within the polymer chain, i.e., $U_{\text{chain}} = NU_{\text{mon}}$. This view has been challenged by Wang et al., based on force-extension curves obtained through single-molecule force spectroscopy (SMFS)[54]. Since U_{mon} is not defined in the case of polymer-like networks, we follow Wang et al. and calculate U_{chain} as the integral of the force-stretch response of a polymer chain[54].

The numerical framework connects strands with behaviors governed by Eq. 5 into a lattice to perform network-level mechanical simulations. We have provided details of the method in our prior works[35,55,56];

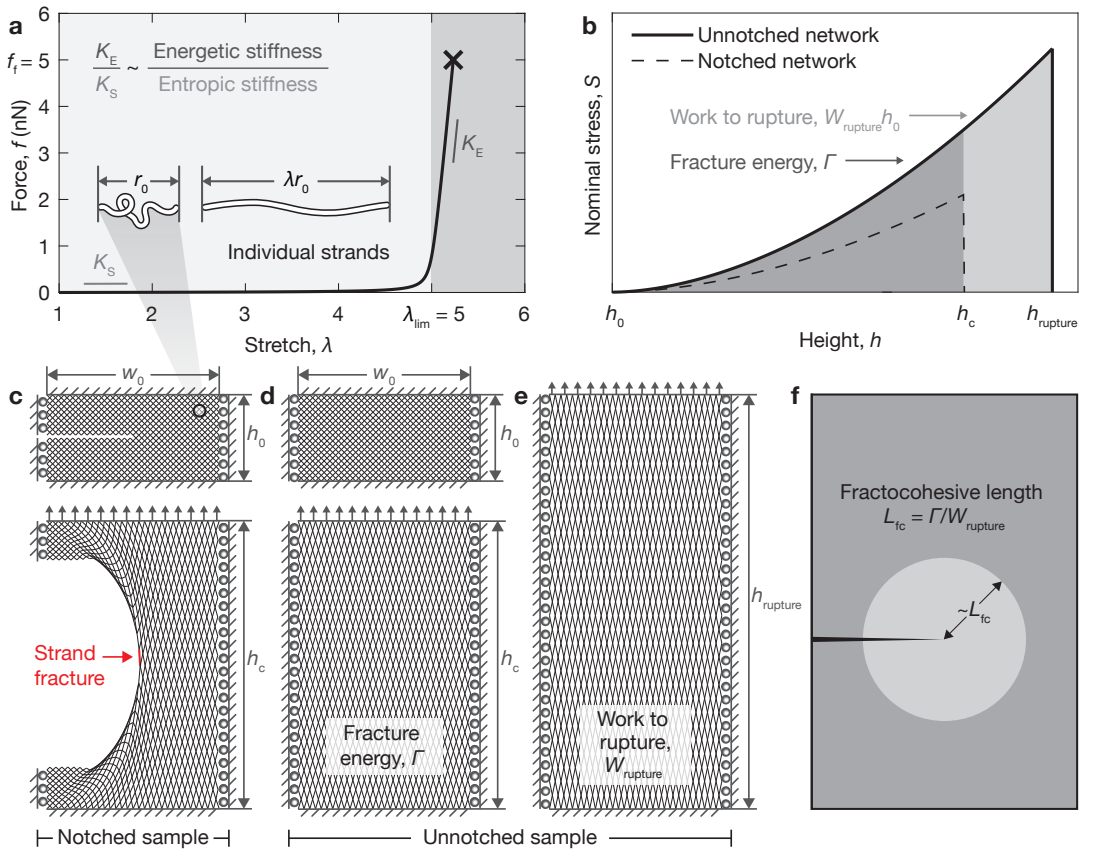

Figure 1. Measuring fractocohesive length in polymer-like networks. (a) Based on single molecule force spectroscopy experiments for a range of flexible polymers[48–53], the nonlinear force-stretch response of polymer chains is modeled by the m-FJC model to transition from entropic unfolding ($\sim K_S$) to bond stretching ($\sim K_E$) at the limiting stretch $\lambda_{lim} = 5$ and break at a fracture force $f_f = 5$ nN. (b) Fracture energy Γ and specific work to rupture $W_{rupture}$ are measured by performing the pure shear fracture test on networks of chains with mechanics governed by the m-FJC model using a quasi-static numerical loading scheme. (c) A notched sample is loaded to the critical height h_c at which the crack propagates by strand fracture. (d) The fracture energy Γ is recorded by loading an unnotched network to h_c. (e) An unnotched sample is loaded to the rupture height $h_{rupture}$ at which the network separates. $W_{rupture}$ is recorded by integrating this response. (f) The fractocohesive length L_{fc} is the ratio of $\Gamma / W_{rupture}$.

here, we outline all loading schemes applied, parameters selected, and adaptations made. Within a collection of nodes and edges, we store the system energy and minimize it stepwise using Newton's method while applying boundary conditions across the network. We track the force applied to displace the network F (via the system energy) as a function of sample height h during quasistatic uniaxial extension

procedures. The nominal stress is defined as the force divided by the cross-sectional area. This gives $S = F/w_0$ in a defect-free 2D lattice with an undeformed width w_0. The model captures failure by removing chains that reach their rupture criteria; it then recalculates the system state for the new network without that chain connection.

We evaluate Γ and W_{rupture} in simulations using two loading schemes (Fig. 1b). We prescribe w_0 to be twice the undeformed height h_0. To measure Γ, we uniaxially extend a notched sample in mode I with an edge crack spanning half of the sample width ($w_0/2$). We record the critical height h_c to propagate the edge crack as the sample height at the maximum sample stress (Fig. 1c). A pristine sample is uniaxially extended from h_0 to the rupture height h_{rupture} where the lattice separates. We record the nominal stress S during the quasistatic loading process as a function of the sample height h to calculate the energy release rate G. Integrating S from the unnotched sample to h_c (Fig. 1d) of the notched sample gives

$$\Gamma = \int_{h_0}^{h_c} S\, dh. \tag{6}$$

We calculate W_{rupture} by integrating the full response of the unnotched sample to h_{rupture} (Fig. 1e) as

$$W_{\text{rupture}} = \frac{1}{h_0} \int_{h_0}^{h_{\text{rupture}}} S\, dh. \tag{7}$$

In perfect highly stretchable networks, the approximation for W_{rupture} as MU_{chain}/L_0 can be applied[57]. Simulations confirm that this result holds for all defect-free polymer-like cases studied here under uniaxial extension with pure shear and tensile loading schemes. Convergence of Γ and W_{rupture} with sample size is ensured by simulating networks with up to 1000 layers of strands, as verified by a convergence study[35]. We coarse-grain the architecture away from stress concentrations in homogeneous regions to improve computational efficiency. By removing a few strands that reach their failure criterion to propagate the crack at the critical energy release rate, simulations indicate that the selected specimen geometry and boundary conditions provide adequate constraints to approximately achieve a change in frame between material behind and ahead of the crack tip. We measure L_{fc} by calculating the dividend of $\Gamma/W_{\text{rupture}}$ from simulations on converged samples (Fig. 1f). The fractocohesive length scales with the size of the region near the crack tip where the material approaches W_{rupture} during fracture. For polymer networks, this measures the extent to which chains approach U_{chain}.

3 Results

We adopt triangular polymer-like networks in two dimensions and measure the fractocohesive length L_{fc} of converged samples while varying the nonlinearity parameter $K_{\text{E}}/K_{\text{S}}$ of the m-FJC model to fit the ranges typical of common polymers. SMFS experiments indicate that poly(acrylic acid) (PAA)[48], poly(vinyl alcohol) (PVA)[49], polyisoprene (*cis*-PI and *trans*-PI)[50], poly(acryl amide) (PAAM)[51], poly(N-isopropyl acrylamide) (PNIPAM)[51], poly(dimethylacrylamide) (PDMA)[52], poly(diethylacrylamide) (PDEA)[52], and poly(ethylene glycol) (PEG)[53] display ratios of $K_{\text{E}}/K_{\text{S}}$ ranging from about 2×10^3 to 2×10^4. The transition stretch $\lambda_{\text{lim}} = 5$ and rupture force $f_{\text{f}} = 5$ nN of chains remain constant. The rupture stretch λ_{f} is solved for using Eq. 5 with a given K_{E} and K_{S}. We calculate the fractocohesive length across this range of polymer-like parameters and find that it exceeds the undeformed mesh size

in all cases (Fig. 2a). Values notably elevate with increasing nonlinearity in chain mechanics (K_E/K_S) up to about 30 times the prediction of the Lake-Thomas model for the case of a network with PEG-like chains ($K_E/K_S \sim 1.8 \times 10^4$).

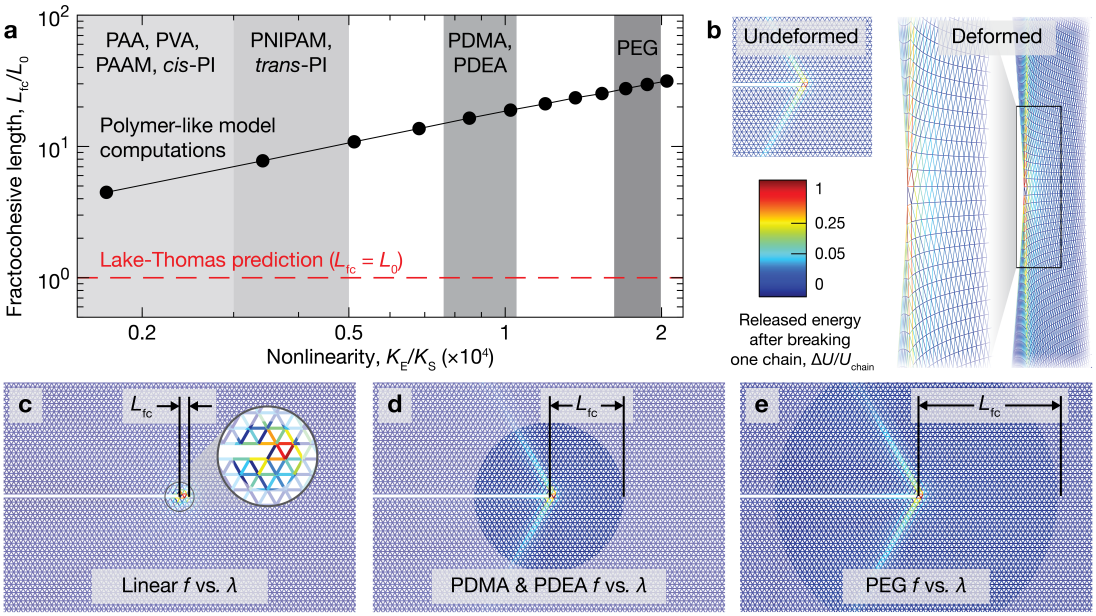

Figure 2. Fractocohesive length of polymer-like networks. (a) The measured fractocohesive length L_{fc} is compared with the undeformed mesh size (Lake-Thomas model) with varying ratios of the nonlinearity parameter K_E/K_S for common polymers. Experimental single-molecular force spectroscopy measurements give the values of K_E and K_S for poly(acrylic acid) (PAA)[48], poly(vinyl alcohol) (PVA)[49], polyisoprene (*cis*-PI and *trans*-PI)[50], poly(acryl amide) (PAAM)[51], poly(N-isopropyl acrylamide) (PNIPAM)[51], poly(dimethylacrylamide) (PDMA)[52], poly(diethylacrylamide) (PDEA)[52], and poly(ethylene glycol) (PEG)[53]. (b) The deformed region near the crack tip of a sample loaded to a stretch of $h_c/h_0 = 2.72$ is mapped onto the undeformed configuration for (c-e) to show the released energy ΔU in each chain after the bridging strand ruptures (normalized by the breaking energy U_{chain}). (c) Networks of strands with linear force-stretch relationship (f vs. λ) display fractocohesive lengths near the undeformed mesh size. Networks of strands parametrized to common polymers like (d) PDMA, PDEA, and (e) PEG give larger fractocohesive lengths.

We analyze chains surrounding the crack tip to further investigate the relationship between the high fractocohesive lengths and the energetic details associated with chain scission. The polymer-like network model enables an in-depth analysis of failure near the tip of the crack by sequentially providing direct mappings of displacements and strain energy distributions throughout the loading procedure. We save the total stored energy U in each chain as a function of the energy to break the chain U_{chain} at each quasistatic loading step p and apply this to calculate the energy change ΔU from steps p to $p+1$ as,

$$\Delta U = L_0 \int_{\lambda^p}^{\lambda^{p+1}} f(\lambda')d\lambda'. \tag{8}$$

Applying this analysis to the steps before and after scission of the bridging strand gives the released energy after breaking one chain. Visualizations can display the released energy for each chain within a region near the crack tip and map these measurements from the deformed to the undeformed configuration, as depicted in Fig. 2b. We perform a control study on a network of strands with linear force-stretch profiles that break at $f_f = 5$ and $\lambda_f = 5$. In Fig. 2c, we display the released energy after breaking the bridging strand at the crack tip of the edge-cracked sample from mode I testing. Fracture and rupture tests indicate that L_{fc} is on the same order as the undeformed mesh size in the network of chains with linear mechanics. We highlight this length scale on the undeformed map with a ring surrounding the bridging chain whose radius equals the magnitude of L_{fc}. Chains releasing pronounced energy are concentrated near the crack tip within this network. We repeat this for networks with chains matching the mechanics of PDMA and PDEA in Fig. 2d and PEG in Fig. 2e. In these polymer-like cases, L_{fc} is larger, and chains releasing significant energy are not concentrated to the few layers surrounding the crack tip. This matches pictures of nonlocal fracture elucidated in computational (discrete, coarse-grained, and continuum)[35,58,59], experimental[5,60,61], and theoretical[6,8,54,62,63] frameworks throughout the literature. The failure zone size near the crack tip–formalized as the dissipative length scale ξ–scales with the fractocohesive length and describes the spatial extent at which the stress and strain concentrations near the tip of the crack decay[10]. Therefore, materials with higher fractocohesive lengths exhibit larger dissipative process zones. We highlight here that the strain-stiffening J-shaped mechanical behavior characteristic of polymer chains with entropic elasticity and bond stretching leads to extraordinarily high values of L_{fc} in polymer-like networks.

Real polymer networks contain defects in the form of dangling ends[6,64], first-order loops[65,66], etc. While network imperfections and inhomogeneities are generally known to increase the value of L_{fc} by orders of magnitude[34], it is difficult to systematically control defects while studying fracture in experiments with real polymers. Similarly, molecular simulations with detailed regulation of defect densities are costly to scale up for bulk fracture simulations containing large cracks. Therefore, due to challenges with conventional measurement techniques, the independent effects of defect size, distribution, and density on the value of L_{fc} remain less understood. We therefore extend the polymer-like simulation platform to model and study networks with defects.

We introduce line defects of length N_{defect} into samples by removing the corresponding edges from the lattice. The values of Γ and $W_{rupture}$ can then be calculated using the same approach as is detailed in Fig. 1 to give L_{fc}. We first conduct a case study on polymer-like networks with defects of chains with nonlinearity $K_E/K_S = 5 \times 10^3$. We fix the defect density ϕ_{defect} to 10% and randomly generate line defects at orientations of 0°, 60°, and 120° to match the topology of the triangular lattice (Fig. 3a). We perform a parallel baseline study on networks with a single dominant defect with the goal of decoupling the roles of defect size and density. We randomly orient and place a defect of length N_{defect} in notched samples and place a centered horizontal defect in unnotched samples as illustrated in Fig. 3b. We perform the loading procedures outlined in Fig. 1 to measure Γ, $W_{rupture}$, and L_{fc} as a function of defect size N_{defect} in sufficiently large networks without coarse-graining (to avoid error from heterogeneities). Recall that the nominal stress S plotted in Fig. 1b for loading of pristine samples is defined for perfect 2D networks as F/w_0. The nominal stress of a sample with a single defect perpendicular to the loading direction can

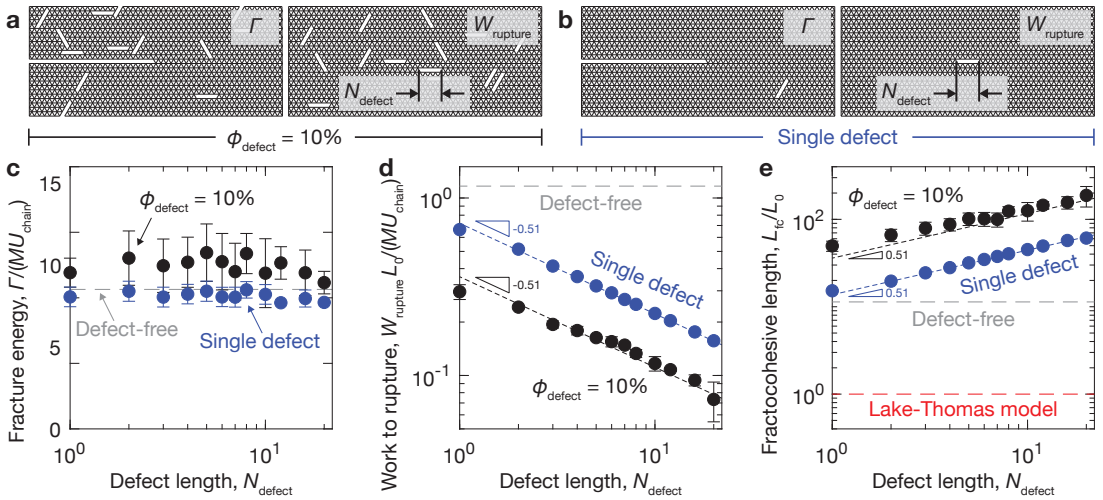

Figure 3. Effect of defect size on the fractocohesive length of polymer-like networks. The fracture energy Γ and specific work to rupture W_{rupture} are measured using notched and unnotched polymer-like networks ($K_{\text{E}}/K_{\text{S}} = 5 \times 10^3$) with (a) a fraction of randomly oriented defects $\phi_{\text{defect}} = 10\%$ of length N_{defect} and compared with (b) notched and unnotched samples with zero defects or a single dominant defect of length N_{defect}. (c) Γ, (d) W_{rupture}, and (e) fractocohesive length L_{fc} (scaled with L_0) are measured as a function of defect length N_{defect}. The best fits for the $\phi_{\text{defect}} = 10\%$ and single defect cases give the same scaling exponent with N_{defect} for (d) specific work to rupture ($W_{\text{rupture}} \sim N_{\text{defect}}^{-0.51}$) and (e) fractocohesive length ($L_{\text{fc}} \sim N_{\text{defect}}^{0.51}$). Error bars depict standard deviations across samples with randomized defect locations and directions.

be defined more generally as $F/(w_0 - N_{\text{defect}}L_0)$ to account for the decrease in elastically active strands. Note that this approach only marginally affects measurements in all cases measured here since the sample widths are much larger than $N_{\text{defect}}L_0$.

Calculations depicted in Fig. 3c indicate that Γ remains approximately constant with respect to defect length at a fixed defect density. We find that this holds for defects whose lengths span less than approximately 10% of the entire sample height used in simulations. Notably, the magnitude of Γ approximately matches the defect-free value. This result holds for networks with $\phi_{\text{defect}} = 10\%$ and those with a single defect. In contrast, increasing the defect length N_{defect} with a fixed defect concentration decreases W_{rupture} (Fig. 3d). While the magnitude of W_{rupture} in the single defect case is higher than the case with 10% defects, the best fit for both cases scale with the same exponent as $W_{\text{rupture}} \sim N_{\text{defect}}^{-0.51}$. The effects of imperfections on the measures of Γ and W_{rupture} interact nonlinearly such that L_{fc} increases with defect density and defect length (Fig. 3e). We fit the fractocohesive length with defect length in the single defect and 10% defects cases and find that they also scale with the same exponent as $L_{\text{fc}} \sim N_{\text{defect}}^{0.51}$.

We further investigate the effect of defects in a range of polymer-like networks by tuning the chain nonlinearity parameter $K_{\text{E}}/K_{\text{S}}$. Results from Fig. 3 motivate the use of Γ from the defect-free case and W_{rupture} from the single defect case to provide a conservative estimate of L_{fc} with respect to the length N_{defect}. We use Γ from the defect-free case because it approximates the magnitude of L_{fc} in cases with

defects without loss of generality. We use W_{rupture} from the single defect case because it gives the same scaling with N_{defect} as the case with random defects. Overall, this strategy results in the same scaling for L_{fc} with N_{defect} as the case with random defects. We apply this approximation technique to measure L_{fc} as a function of defect length while varying $K_{\text{E}}/K_{\text{S}}$. Computations indicate that the fractocohesive length can exceed the undeformed mesh size by over two orders of magnitude in polymer-like networks with defects (Fig. 4a). We normalize this result by the fractocohesive length of the defect-free sample $L_{\text{fc}}^{\text{defect-free}}$ with the same $K_{\text{E}}/K_{\text{S}}$ in Fig. 4b. We find that the power-law scaling with N_{defect} decreases as the nonlinearity parameter $K_{\text{E}}/K_{\text{S}}$ increases from $L_{\text{fc}} \sim N_{\text{defect}}^{0.80}$ for $K_{\text{E}}/K_{\text{S}} = 1.0 \times 10^3$ to $L_{\text{fc}} \sim N_{\text{defect}}^{0.34}$ for $K_{\text{E}}/K_{\text{S}} = 1.8 \times 10^4$.

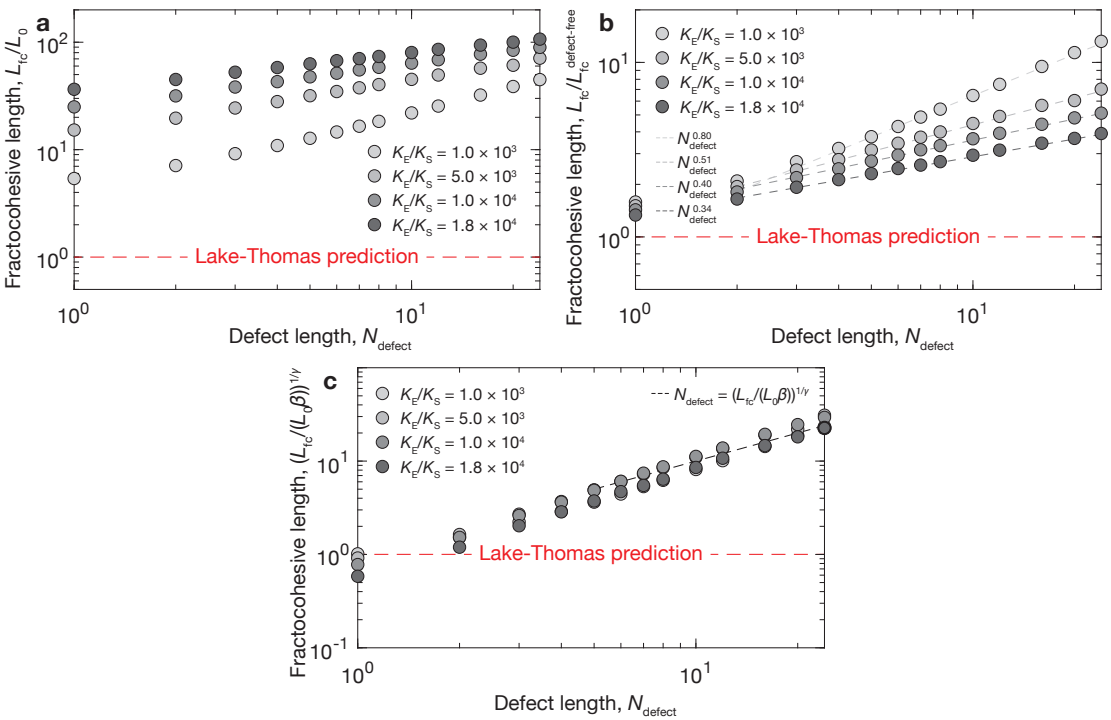

Figure 4. Scaling for fractocohesive length in polymer-like networks with defects. (a) The variation in fractocohesive length L_{fc} with respect to defect length N_{defect} for varying nonlinearity ratios $K_{\text{E}}/K_{\text{S}}$ is conservatively approximated by the defect-free fracture energy and the specific work to rupture W_{rupture} of a sample with one dominant defect since the ordering of these values capture the general order of magnitude and ordering of L_{fc}. (b) The scaling of L_{fc} with $K_{\text{E}}/K_{\text{S}}$ when normalized by the defect-free case $L_{\text{fc}}^{\text{defect-free}}$. The legend displays the best fit power law scaling for a range of values of $K_{\text{E}}/K_{\text{S}}$. (c) The outcome of normalizing L_{fc} by the proposed scaling formalized in Eq. 9 and plotting results with respect to N_{defect} for $N_{\text{defect}} \geq 5$. The scaling relationship predicts that results will collapse to a linear trend on double logarithmic axes (dashed black line).

We now propose a scaling relationship based on these conclusions that predicts the fractocohesive length of perfect and imperfect polymer-like networks. By analyzing how the fractocohesive length scales with each parameter from calculations, the model attempts to resolve contributions from strand mechanics and defects of various size. Results indicate that strand nonlinearity $K_{\mathrm{E}}/K_{\mathrm{S}}$ and defect length N_{defect} each affect the fractocohesive length in polymer-like systems. We assume the case of a single defect and find that fractocohesive length L_{fc} relates to the undeformed mesh size L_0 as,

$$L_{\mathrm{fc}} = \beta N_{\mathrm{defect}}^{\gamma} L_0, \tag{9}$$

where the parameter β describes the effect of strain-stiffening in chains and the power law exponent γ describes the scaling with defect length. Note from Fig. 4b that the scaling with γ depends on $K_{\mathrm{E}}/K_{\mathrm{S}}$ and, therefore, is coupled with the nonlinear mechanics of the chain deformation. We can determine relationships for β and γ based on the numerical results. We find that β can be written as,

$$\beta = \frac{\alpha f_{\mathrm{f}} \lambda_{\mathrm{f}}}{U_{\mathrm{chain}}}, \tag{10}$$

where α is a geometric parameter describing the lattice topology in 2D and 3D networks ($\alpha = 0.73$ for a 2D triangular lattice) that relates to loop size[55]. Note that β directly encodes the effects of strain-stiffening; β increases with $K_{\mathrm{E}}/K_{\mathrm{S}}$ in networks of polymer-like chains (see Fig. 4a). We find that γ can be written as a function of β by fitting results, giving,

$$\gamma = (2/\beta)^{0.4}. \tag{11}$$

for the triangular lattice topology tested here. Note that Eq. 9 applies for networks containing defects of a finite size; the defect-free case should instead be modeled using $L_{\mathrm{fc}} = \beta L_0$. We normalize the fractocohesive length L_{fc} by the scaling framework presented in Eq. 9 and plot simulation results against defect length N_{defect} in Fig. 4c to demonstrate the applicability of the model to networks with $N_{\mathrm{defect}} \geq 5$. We suspect that geometric effects can account for deviations from the model in predicting results for networks with $N_{\mathrm{defect}} < 5$. This result highlights how implementing the J-shaped force-extension curve of Eq. 5 that is typical of real polymer chains elevates the fractocohesive length well beyond the undeformed mesh size in perfect networks. Imperfections serve to further increase this ratio. We capture the effect of defect length through the exponent γ. The proposed model provides insights into the roles of polymer-like chains and defects in amplifying length scales involved in soft network fracture.

4 Conclusion

This work raises several open and ongoing questions regarding fracture of polymer and polymer-like networks. For example, subsequent work must be done to fully interpret the physics that underpins the scaling results determined computationally here. Other topological and architectural details that are common in real polymer networks also warrant further analysis, such as chain entanglements[25], interpenetrating networks[21], and polydispersity[67]. More complex damage models incorporating additional volumetric, temporal, and diffusive effects relevant to many real polymer networks could help to address these questions. Results from this work could also have implications

for improving gradient-enhanced[58,68–70] and cohesive zone[71–73] fracture models incorporating nonlocal effects. Overall, studying material-specific length scales relevant to fracture through polymer-like network models provides an efficient yet robust computational platform to shed light on the fundamental nonlinear chain mechanics that govern these important problems.

In summary, we show that perfect, defect-free polymer-like networks exhibit fractocohesive lengths that far surpass their undeformed mesh sizes, deviating from the prediction of the Lake-Thomas model. We measure this by performing fracture tests in the limit of small and large cracks on pure shear specimens using a computational polymer-like network model to characterize the fractocohesive length with accurately calibrated molecular mechanics and architectures. Calculations demonstrate that the fractocohesive length exceeds the mesh size by an order of magnitude in networks composed of chains with nonlinear force-extension curves matching the performance of common polymers. We find that it increases when the strain-stiffening force-stretch behavior of chains is more pronounced (i.e., with increasing $K_{\mathrm{E}}/K_{\mathrm{S}}$). In these notched samples, the energy dissipated by chains during crack growth far outweighs the energy consumed in breaking a layer of strands. Chains exhibiting significant energy release disseminate well beyond the tip of the crack. Dynamic simulations indicate that this promotes a larger energy dissipation zone[35]. Adding imperfections through defects of varying density and size further amplifies these results. In particular, for a given defect density, we demonstrate that the fractocohesive length grows as a function of the defect length. Evidence suggests that these findings can be rationalized by augmenting the prediction of the Lake-Thomas model by incorporating scalings given by Eqs. 9-11. We propose a modified model that relates the fractocohesive length of polymer-like networks to the mechanics of chain extension, the topology of the network architecture, and the length of defects at a given defect density. Our study highlights important molecular details, such as the nonlinear chain force-extension curve along with the number and size of defects in the sample, which promote fracture resistance in polymer networks. It also provides a computationally efficient approach to modeling fractocohesive lengths of diverse elastomeric networks across scales. Our findings not only shed light on soft, tough, and stretchable polymer network design principles but provide direct implications for developing fatigue-resistant biomaterials and metamaterials for use in domains such as healthcare, aerospace, and soft robotics.

Acknowledgements

The authors acknowledge the MIT SuperCloud and Lincoln Laboratory Supercomputing Center for providing HPC resources that have contributed to the research results reported within this paper.

Declaration of conflicting interests

The authors declared no potential conflicts of interest with respect to the research, authorship, and/or publication of this article.

Funding

This work was supported in part by the National Institutes of Health (Grants No. 1R01HL153857-01 and No. 1R01HL167947-01), Department of Defense Congressionally Directed Medical Research Programs (Grant No. PR200524P1), and the National Science Foundation (Grant No. EFMA-1935291). The authors also acknowledge support from startup funds through the University of Florida.

References

1. Creton C and Ciccotti M. Fracture and adhesion of soft materials: a review. *Reports on Progress in Physics* 2016; 79(4): 046601.
2. Zhao X, Chen X, Yuk H et al. Soft materials by design: unconventional polymer networks give extreme properties. *Chemical Reviews* 2021; 121(8): 4309–4372.
3. Xu C, Chen Y, Zhao S et al. Mechanical regulation of polymer gels. *Chemical Reviews* 2024; 124(18): 10435–10508.
4. Griffith AA. VI. the phenomena of rupture and flow in solids. *Philosophical Transactions of the Royal Society of London Series A, Containing Papers of a Mathematical or Physical Character* 1921; 221(582-593): 163–198.
5. Livne A, Bouchbinder E, Svetlizky I et al. The near-tip fields of fast cracks. *Science* 2010; 327(5971): 1359–1363.
6. Lin S and Zhao X. Fracture of polymer networks with diverse topological defects. *Physical Review E* 2020; 102(5): 052503.
7. Akagi Y, Gong JP, Chung UI et al. Transition between phantom and affine network model observed in polymer gels with controlled network structure. *Macromolecules* 2013; 46(3): 1035–1040.
8. Barney CW, Ye Z, Sacligil I et al. Fracture of model end-linked networks. *Proceedings of the National Academy of Sciences* 2022; 119(7): e2112389119.
9. Wang S, Beech HK, Bowser BH et al. Mechanism dictates mechanics: a molecular substituent effect in the macroscopic fracture of a covalent polymer network. *Journal of the American Chemical Society* 2021; 143(10): 3714–3718.
10. Long R, Hui CY, Gong JP et al. The fracture of highly deformable soft materials: A tale of two length scales. *Annual Review of Condensed Matter Physics* 2021; 12: 71–94.
11. Chen C, Wang Z and Suo Z. Flaw sensitivity of highly stretchable materials. *Extreme Mechanics Letters* 2017; 10: 50–57.
12. Thomas A. Rupture of rubber. II. The strain concentration at an incision. *Journal of Polymer Science* 1955; 18(88): 177–188.
13. Volokh K and Trapper P. Fracture toughness from the standpoint of softening hyperelasticity. *Journal of the Mechanics and Physics of Solids* 2008; 56(7): 2459–2472.
14. Gao H, Ji B, Jäger IL et al. Materials become insensitive to flaws at nanoscale: lessons from nature. *Proceedings of the National Academy of Sciences* 2003; 100(10): 5597–5600.
15. Zhang T, Li X, Kadkhodaei S et al. Flaw insensitive fracture in nanocrystalline graphene. *Nano letters* 2012; 12(9): 4605–4610.
16. Lake G and Lindley P. The mechanical fatigue limit for rubber. *Journal of Applied Polymer Science* 1965; 9(4): 1233–1251.
17. Zeng L, Liu F, Yu Q et al. Flaw-insensitive fatigue resistance of chemically fixed collagenous soft tissues. *Science Advances* 2023; 9(9): eade7375.
18. Ma J, Zhang X, Yin D et al. Designing ultratough single-network hydrogels with centimeter-scale fractocohesive lengths via inelastic crack blunting. *Advanced Materials* 2024; 36(23): 2311795.
19. Han Z, Wang P, Lu Y et al. A versatile hydrogel network–repairing strategy achieved by the covalent-like hydrogen bond interaction. *Science Advances* 2022; 8(8): eabl5066.
20. Thomas A. Rupture of rubber. V. Cut growth in natural rubber vulcanizates. *Journal of Polymer Science* 1958; 31(123): 467–480.

Accepted version. Published in *Mathematics and Mechanics of Solids.*

21. Gong JP, Katsuyama Y, Kurokawa T et al. Double-network hydrogels with extremely high mechanical strength. *Advanced Materials* 2003; 15(14): 1155–1158.
22. Haque MA, Kurokawa T, Kamita G et al. Lamellar bilayers as reversible sacrificial bonds to toughen hydrogel: hysteresis, self-recovery, fatigue resistance, and crack blunting. *Macromolecules* 2011; 44(22): 8916–8924.
23. Sun JY, Zhao X, Illeperuma WR et al. Highly stretchable and tough hydrogels. *Nature* 2012; 489(7414): 133–136.
24. Ducrot E, Chen Y, Bulters M et al. Toughening elastomers with sacrificial bonds and watching them break. *Science* 2014; 344(6180): 186–189.
25. Kim J, Zhang G, Shi M et al. Fracture, fatigue, and friction of polymers in which entanglements greatly outnumber cross-links. *Science* 2021; 374(6564): 212–216.
26. Wu X, Li X, Sun S et al. Fracture process zone and fracture energy of heterogeneous soft materials. *Journal of the Mechanics and Physics of Solids* 2025; 196: 105997.
27. Chen Q, Chen B, Jing S et al. Flaw sensitivity of cellulose paper. *Extreme Mechanics Letters* 2022; 56: 101865.
28. Hartquist CM, Lin S, Zhang JH et al. An elastomer with ultrahigh strain-induced crystallization. *Science Advances* 2023; 9(50): eadj0411.
29. Li C, Wang Z, Wang Y et al. Effects of network structures on the fracture of hydrogel. *Extreme Mechanics Letters* 2021; 49: 101495.
30. Persson B and Brener E. Crack propagation in viscoelastic solids. *Physical Review E—Statistical, Nonlinear, and Soft Matter Physics* 2005; 71(3): 036123.
31. Song Z, Shen T, Vernerey FJ et al. Force-dependent bond dissociation explains the rate-dependent fracture of vitrimers. *Soft Matter* 2021; 17(27): 6669–6674.
32. Zheng Y, Matsuda T, Nakajima T et al. How chain dynamics affects crack initiation in double-network gels. *Proceedings of the National Academy of Sciences* 2021; 118(49): e2111880118.
33. Lavoie SR and Suo Z. Flaw sensitivity of stochastic elastic materials. *Mathematics and Mechanics of Solids* 2024; 29(6): 1228–1238.
34. Yang C, Yin T and Suo Z. Polyacrylamide hydrogels. I. Network imperfection. *Journal of the Mechanics and Physics of Solids* 2019; 131: 43–55.
35. Deng B, Wang S, Hartquist C et al. Nonlocal intrinsic fracture energy of polymerlike networks. *Physical Review Letters* 2023; 131(22): 228102.
36. Lei J, Li Z, Xu S et al. A mesoscopic network mechanics method to reproduce the large deformation and fracture process of cross-linked elastomers. *Journal of the Mechanics and Physics of Solids* 2021; 156: 104599.
37. Ghareeb A and Elbanna A. An adaptive quasicontinuum approach for modeling fracture in networked materials: Application to modeling of polymer networks. *Journal of the Mechanics and Physics of Solids* 2020; 137: 103819.
38. Lei J and Liu Z. A network mechanics method to study the mechanism of the large-deformation fracture of elastomers. *Journal of Applied Physics* 2022; 132(13).
39. Arora A. Effect of spatial heterogeneity on the elasticity and fracture of polymer networks. *Macromolecules* 2025; 58(2): 1143–1155.
40. Picu R and Jin S. Toughness of network materials: Structural parameters controlling damage accumulation. *Journal of the Mechanics and Physics of Solids* 2023; 172: 105176.
41. Yamaguchi T, Onoue Y and Sawae Y. Topology and toughening of sparse elastic networks. *Physical Review Letters* 2020; 124(6): 068002.

42. Pan Z, Ma R, Wang D et al. A review of lattice type model in fracture mechanics: theory, applications, and perspectives. *Engineering Fracture Mechanics* 2018; 190: 382–409.
43. Broedersz CP and MacKintosh FC. Modeling semiflexible polymer networks. *Reviews of Modern Physics* 2014; 86(3): 995.
44. Kuhn W. Dependence of the average transversal on the longitudinal dimensions of statistical coils formed by chain molecules. *Journal of Polymer Science* 1946; 1(5): 380–388.
45. Smith SB, Cui Y and Bustamante C. Overstretching B-DNA: the elastic response of individual double-stranded and single-stranded DNA molecules. *Science* 1996; 271(5250): 795–799.
46. Mao Y and Anand L. A theory for fracture of polymeric gels. *Journal of the Mechanics and Physics of Solids* 2018; 115: 30–53.
47. Buche MR, Silberstein MN and Grutzik SJ. Freely jointed chain models with extensible links. *Physical Review E* 2022; 106(2): 024502.
48. Li H, Liu B, Zhang X et al. Single-molecule force spectroscopy on poly (acrylic acid) by AFM. *Langmuir* 1999; 15(6): 2120–2124.
49. Li H, Zhang W, Zhang X et al. Single molecule force spectroscopy on poly (vinyl alcohol) by atomic force microscopy. *Macromolecular Rapid Communications* 1998; 19(12): 609–611.
50. Zhang W. *Nano-mechanical detection of single molecules*. PhD Thesis, Jilin University, 2002.
51. Zhang W, Zou S, Wang C et al. Single polymer chain elongation of poly (n-isopropylacrylamide) and poly (acrylamide) by atomic force microscopy. *The Journal of Physical Chemistry B* 2000; 104(44): 10258–10264.
52. Wang C, Shi W, Zhang W et al. Force spectroscopy study on poly (acrylamide) derivatives: Effects of substitutes and buffers on single-chain elasticity. *Nano Letters* 2002; 2(10): 1169–1172.
53. Oesterhelt F, Rief M and Gaub H. Single molecule force spectroscopy by AFM indicates helical structure of poly (ethylene-glycol) in water. *New Journal of Physics* 1999; 1(1): 6.
54. Wang S, Panyukov S, Rubinstein M et al. Quantitative adjustment to the molecular energy parameter in the Lake–Thomas theory of polymer fracture energy. *Macromolecules* 2019; 52(7): 2772–2777.
55. Hartquist C, Wang S, Cui Q et al. Scaling law for intrinsic fracture energy of diverse stretchable networks. *Physical Review X* 2025; 15(1): 011002.
56. Hartquist CM, Wang S, Deng B et al. Fracture of polymer-like networks with hybrid bond strengths. *Journal of the Mechanics and Physics of Solids* 2025; 195: 105931.
57. Orowan E. Fracture and strength of solids. *Reports on Progress in Physics* 1949; 12(1): 185.
58. Talamini B, Mao Y and Anand L. Progressive damage and rupture in polymers. *Journal of the Mechanics and Physics of Solids* 2018; 111: 434–457.
59. Mousavi SM, Mulderrig J, Talamini B et al. A chain stretch-based gradient-enhanced model for damage and fracture in elastomers. *Computer Methods in Applied Mechanics and Engineering* 2025; 444: 118103.
60. Xue N, Long R, Dufresne ER et al. Elastomers fail from the edge. *Physical Review X* 2024; 14(1): 011054.
61. Lu W, Wang C, Zhou Z et al. Quantify the failure zone and elastic release zone: A new insight into intrinsic fracture of polymer networks. *Extreme Mechanics Letters* 2025; 78: 102362.
62. Wang S, Panyukov S, Craig SL et al. Contribution of unbroken strands to the fracture of polymer networks. *Macromolecules* 2023; 56(6): 2309–2318.
63. Wang S, Hartquist CM, Deng B et al. A loop-opening model for the intrinsic fracture energy of polymer networks. *Macromolecules* 2024; 57(13): 6069–6075.
64. Di Lorenzo F and Seiffert S. Nanostructural heterogeneity in polymer networks and gels. *Polymer Chemistry* 2015; 6(31): 5515–5528.

65. Zhou H, Woo J, Cok AM et al. Counting primary loops in polymer gels. *Proceedings of the National Academy of Sciences* 2012; 109(47): 19119–19124.
66. Panyukov S. Loops in polymer networks. *Macromolecules* 2019; 52(11): 4145–4153.
67. Arora A, Lin TS, Beech HK et al. Fracture of polymer networks containing topological defects. *Macromolecules* 2020; 53(17): 7346–7355.
68. Lorentz E and Godard V. Gradient damage models: Toward full-scale computations. *Computer Methods in Applied Mechanics and Engineering* 2011; 200(21-22): 1927–1944.
69. Vernerey FJ, Brighenti R, Long R et al. Statistical damage mechanics of polymer networks. *Macromolecules* 2018; 51(17): 6609–6622.
70. Mulderrig J, Li B and Bouklas N. Affine and non-affine microsphere models for chain scission in polydisperse elastomer networks. *Mechanics of Materials* 2021; 160: 103857.
71. Elices M, Guinea G, Gomez J et al. The cohesive zone model: advantages, limitations and challenges. *Engineering fracture mechanics* 2002; 69(2): 137–163.
72. Park K and Paulino GH. Cohesive zone models: a critical review of traction-separation relationships across fracture surfaces. *Applied Mechanics Reviews* 2011; 64(6): 060802.
73. Hui C, Ruina A, Long R et al. Cohesive zone models and fracture. *The Journal of Adhesion* 2011; 87(1): 1–52.